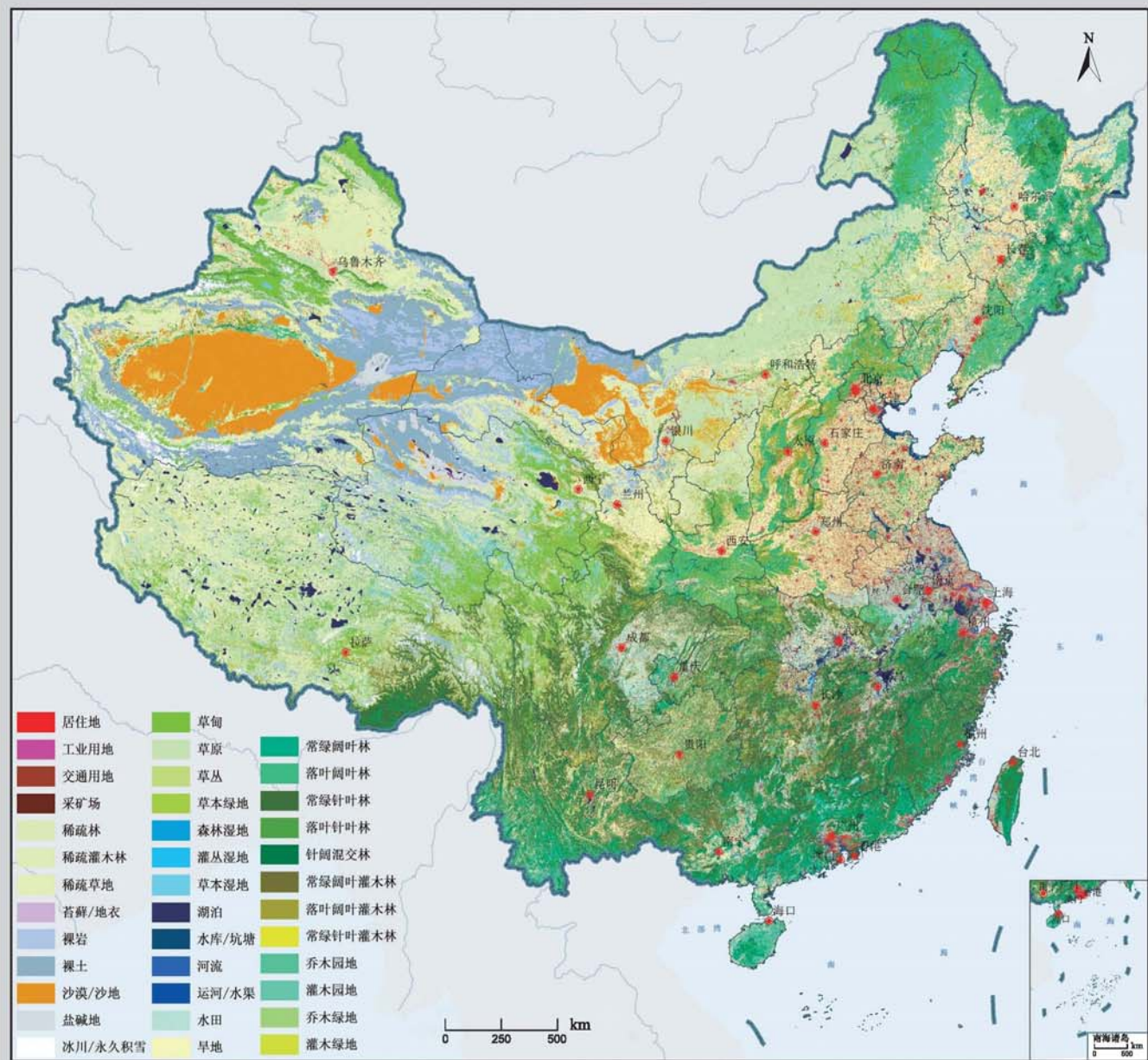


2010年中国土地覆被遥感监测数据集 (ChinaCover2010)





遥感学报

Yaogan Xuebao

第 17 卷 第 4 期 2013 年 7 月

目 次

综述

森林垂直结构参数遥感反演综述 赵静, 李静, 柳钦火 (707)

基础理论

HASM 解算的 2 维双连续投影方法 闫长青, 岳天祥, 赵刚, 王晨亮 (722)

地形起伏度最佳分析区域预测模型 张锦明, 游雄 (735)

技术方法

运用 GVF Snake 算法提取水域的不规则边界 朱述龙, 孟伟灿, 朱宝山 (750)

全景立体视觉的快速近区重力地形改正方法 邸凯昌, 吴凯, 刘召芹, 万文辉, 邸志众, 李钢 (767)

利用氧气和水汽吸收波段暗像元假设的 MERIS 影像二类水体大气校正方法

..... 檀静, 李云梅, 赵运林, 吕恒, 徐德强, 周莉, 刘阁 (778)

自然语言理解的中文地址匹配算法 宋子辉 (795)

3 维地形的金字塔上下采样局部实时简化算法 易雄鹰, 方超 (809)

面向对象分类特征优化选取方法及其应用 王贺, 陈劲松, 余晓敏 (822)

针对 Terra/MODIS 数据的改进分裂窗地表温度反演算法

..... RI Changin, 柳钦火, 厉华, 方莉, YU Yunyue, SUN Donglian (840)

基于 Voronoi 几何划分和 EM/MPM 算法的多视 SAR 图像分割 赵泉华, 李玉, 何晓军, 宋伟东 (847)

遥感应用

地面成像光谱数据的田间杂草识别 李颖, 张立福, 严薇, 黄长平, 童庆禧 (863)

耦合遥感观测和元胞自动机的城市扩张模拟 张亦汉, 黎夏, 刘小平, 乔纪纲, 何执兼 (879)

结合凝聚层次聚类的极化 SAR 海冰分割 于波, 孟俊敏, 张晰, 纪永刚 (896)

杭州湾 HJ CCD 影像悬浮泥沙遥感定量反演 刘王兵, 于之锋, 周斌, 蒋锦刚, 潘玉良, 凌在盈 (912)

“灰霾遥感”专栏

北京区域 2013 严重灰霾污染的主被动遥感监测

..... 李正强, 许华, 张莹, 张玉环, 陈澄, 李东辉, 李莉, 侯伟真, 吕阳, 顾行发 (924)

利用细模态气溶胶光学厚度估计 $PM_{2.5}$ 张莹, 李正强 (936)

利用太阳-天空辐射计遥感观测反演北京冬季灰霾气溶胶成分含量

..... 王玲, 李正强, 马䶮, 李莉, 魏鹏 (951)

利用 HJ-1 CCD 高分辨率传感器反演灰霾气溶胶光学厚度 张玉环, 李正强, 侯伟真, 许华 (964)

基于地基遥感的灰霾气溶胶光学及微物理特性观测

..... 谢一淞, 李东辉, 李凯涛, 张龙, 陈澄, 许华, 李正强 (975)

利用激光雷达探测灰霾天气大气边界层高度 张婉春, 张莹, 吕阳, 李凯涛, 李正强 (987)

北京区域冬季灰霾过程中人为气溶胶光学厚度估算 王堰, 谢一淞, 李正强, 李东辉, 李凯涛 (1000)

结合地基激光雷达和太阳辐射计的气溶胶垂直分布观测

..... 吕阳, 李正强, 尹鹏飞, 许华, 李凯涛, 张婉春, 侯伟真 (1014)

灰霾污染状况下气溶胶组分及辐射效应的遥感估算

..... 魏鹏, 李正强, 王堰, 谢一淞, 张莹, 许华 (1026)

JOURNAL OF REMOTE SENSING

(Vol. 17 No. 4 July, 2013)

CONTENTS

Review

- Review of forest vertical structure parameter inversion based on remote sensing technology
..... ZHAO Jing, LI Jing, LIU Qinhuo (697)

Fundamental Research

- Two-dimensional double successive projection method for high accuracy surface modeling
..... YAN Changqing, YUE Tianxiang, ZHAO Gang, WANG Chenliang (717)
- A prediction model of optimum statistical unit of relief ZHANG Jinming, YOU Xiong (728)

Technology and Methodology

- Irregular water boundary extraction using GVF snake ZHU Shulong, MENG Weican, ZHU Baoshan (742)
- Fast near-region gravity terrain correction approach based on panoramic stereo vision
..... DI Kaichang, WU Kai, LIU Zhaoqin, WAN Wenhui, DI Zhizhong, LI Gang (759)
- Atmospheric correction of MERIS data on the black pixel assumption in oxygen and water vapor absorption
bands TAN Jing, LI Yunmei, Zhao Yunlin, LV Heng, XU Deqiang, ZHOU Li, LIU Ge (768)
- Address matching algorithm based on chinese natural language understanding SONG Zihui (788)
- Local real-time simplification algorithm for three-dimensional terrain using up and down sampling and
pyramid theory YI Xiongying, FANG Chao (802)
- Feature selection and its application in object-oriented classification
..... WANG He, CHEN Jinsong, YU Xiaomin (816)
- Improved split window algorithm to retrieve LST from Terra/MODIS data
..... RI Changin, LIU Qinhuo, LI Hua, FANG Li, YU Yunyue, SUN Donglian (830)
- Multi-look SAR image segmentation based on voronoi tessellation technique and EM/MPM algorithm
..... ZHAO Quanhua, LI Yu, HE Xiaojun, SONG Weidong (841)

Remote Sensing Applications

- Weed identification using imaging spectrometer data
..... LI Ying, ZHANG Lifu, YAN Wei, HUANG Changping, TONG Qingxi (855)
- Urban expansion simulation by coupling remote sensing observations and cellular automata
..... ZHANG Yihan, LI Xia, LIU Xiaoping, QIAO Jigang, HE Zhijian (872)
- Segmentation method for agglomerative hierarchical-based sea ice types using polarimetric SAR data
..... YU Bo, MENG Junmin, ZHANG Xi, JI Yonggang (887)
- Assessment of suspended sediment concentration at the Hangzhou Bay using HJ CCD imagery
..... LIU Wangbing, YU Zhifeng, ZHOU Bin, JIANG Jingang, PAN Yuliang, LING Zaiying (905)

(to be continued to Inside Back Cover)

(continued from Contents page)

Haze: Remote Sensing

- Joint use of active and passive remote sensing for monitoring of severe haze pollution in Beijing 2013 *LI Zhengqiang, XU Hua, ZHANG Ying, ZHANG Yuhuan, CHEN Cheng, LI Donghui, LI Li, HOU Weizhen, LV Yang, GU Xingfa* (919)
- Estimation of PM_{2.5} from fine-mode aerosol optical depth *ZHANG Ying, LI Zhengqiang* (929)
- Retrieval of aerosol chemical composition from ground-based remote sensing data of sun-sky radiometers during haze days in Beijing winter *WANG Ling, LI Zhengqiang, MA Yan, LI Li, WEI Peng* (944)
- Retrieval of haze aerosol optical depth based on high spatial resolution CCD of HJ-1 *ZHANG Yuhuan, LI Zhengqiang, HOU Weizhen, XU hua* (959)
- Aerosol optical and microphysical properties in haze days based on ground-based remote sensing measurements *XIE Yisong, LI Donghui, LI Kaitao, ZHANG Long, CHEN Cheng, XU Hua, LI Zhengqiang* (970)
- Observation of atmospheric boundary layer height by ground-based LiDAR during haze days *ZHANG Wanchun, ZHANG Ying, LV Yang, LI Kaitao, LI Zhengqiang* (981)
- Anthropogenic aerosol optical depth during days of high haze levels in the Beijing winter *WANG Yan, XIE Yisong, LI Zhengqiang, LI Donghui, LI Kaitao* (993)
- Joint use of ground-based LiDAR and sun-sky radiometer for observation of aerosol vertical distribution *LV Yang, LI Zhengqiang, YIN Pengfei, XU Hua, LI Kaitao, ZHANG Wanchun, HOU Weizhen* (1008)
- Remote sensing estimation of aerosol composition and radiative effects in haze days *WEI Peng, LI Zhengqiang, WANG Yan, XIE Yisong, ZHANG Ying, XU Hua* (1021)

Two-dimensional double successive projection method for high accuracy surface modeling

YAN Changqing^{1,2}, YUE Tianxiang¹, ZHAO Gang¹, WANG Chenliang¹

1. State Key Laboratory of Resources and Environment Information System, Jointly Sponsored by Institute of Geographic Science and Natural Resources Research of Chinese Academy of Sciences, Beijing 100101, China;
2. Department of Information Engineering, Shandong University of Science and Technology, Tai'an 271000, China

Abstract: High Accuracy Surface Modeling (HASM) method, based on the fundamental theorem of surfaces, provides a solution to the error problem that long troubled geographic information science. Although HASM has a sound theoretical foundation, the low computing efficiency arising from solving large scale linear systems, poses a severe limitation on its wide-spread applications in construction of large scale and high resolution surfaces. In order to achieve a high speed, we developed an algorithm based on two dimensional Double Successive Projection Method (HASM-DSPM), which significantly improves the performance by adopting strategies of project space adjustment and two-step correction. HASM-DSPM is examined by both numerical experiment and real world experiment, the results of which both illustrate that HASM can surpass Gauss-Seidel (GS) and Modified GS (MGS) in convergence pace and computational speed. Furthermore, compared with other classical surface modeling methods, our method has obviously higher accuracy.

Key words: HASM, two-dimensional double successive projection, surface simulation, MGS iteration, DEM

CLC number: TP751.1 **Document code:** A

Citation format: Yan C Q, Yue T X, Zhao G and Wang C L. 2013. Two-dimensional double successive projection method for high accuracy surface modeling. Journal of Remote Sensing, 17(4): 717-727 [DOI: 10.11834/jrs.20132206]

1 INTRODUCTION

Surface simulation has been widely applied in the simulation of overall aspects of earth surface, ranging from climate simulation (Zhou, et al., 2012), ecological simulation (Chen, et al., 2012; Shi, et al., 2009) to Digital Elevation Model (DEM) construction (Yue, 2011). Generally, surface simulation involves three stages: surface sampling, surface simulation employing numerical methods, evaluation of simulated surface (Hengl & Evans, 2009). Due to lack of complete theoretical foundation, current surface simulation methods can yield products with serious error even incorrect results when used to simulate surface. In order to solve the error problem, high accuracy surface modeling method is presented and developed (Yue, et al., 2004; Yue & Du, 2006; Yue, 2011), which is based on differential geometry and solves the error problem that long troubled Geographic Information Science (GIS). Although this method is mature theoretically, the low speed arising from the solution of huge linear system constrains its applications in real-

time, large scale and high resolution simulation. To improve the computing efficiency, Yue, et al. (2008) employed a multi-grid method for solving the large linear system of HASM and found that multi-grid method can be well adapted for large scale simulation; Chen, et al. (2012) proposed a modified Gauss-Seidel method to further improve the efficiency of construction of the DEM with HASM. This method accelerated the construction of DEM while maintaining the high accuracy. Furthermore, it consumed less memory and hence can be adopted for large scale DEM simulation.

Based on the investigation of the method of Chen, et al. (2012), this paper introduces the spatial projection technique to solve the linear system of HASM, and hence to present a new method based on two dimensional double successive projection (HASM-DSPM). Subsequently, the method is validated through simulation of Gauss synthetic surface and real-world example. Finally, conclusions are drawn in the last section.

Received: 2012-07-03; **Accepted:** 2012-10-17; **Version of record first published:** 2012-10-24

Foundation: National Science Fund for Distinguished Young Scholars of China (No.40825003); National High Technology Research and Development Program (863 Program) (No.2011AA120306); Young and Middle-Aged Scientists Research Awards Fund of Shandong Province (No. BS2012HZ010); Spring Buds Program of Shandong University of Science and Technology (No.2010AZZ115)

First author biography: YAN Changqing (1978—), male, Ph.D. candidate, he majors in resources and environmental models and system simulation.
E-mail: yancq@lreis.ac.cn

Corresponding author biography: YUE Tianxiang (1943—), male, professor. His research interest is earth surface modeling. E-mail:yue@lreis.ac.cn

2 TWO-DIMENSIONAL DOUBLE SUCCESSIVE PROJECTION BASED HASM METHOD

2.1 High accuracy surface modeling method

HASM is based on the fundamental theorem of surfaces in principles of differential geometry. In terms of the unique deterministic factor of surface, HASM method converts the surface modeling task to the solution of partial differential equation group following

$$\begin{cases} f_{xx} = \Gamma_{11}^1 \cdot f_x + \Gamma_{11}^2 \cdot f_y + L \cdot (E \cdot G - F^2)^{-1/2} \\ f_{yy} = \Gamma_{22}^1 \cdot f_x + \Gamma_{22}^2 \cdot f_y + N \cdot (E \cdot G - F^2)^{-1/2} \end{cases} \quad (1)$$

where $E = 1 + f_x^2$, $F = f_x \cdot f_y$, $G = 1 + f_y^2$, $L = \frac{f_{xx}}{\sqrt{1 + f_x^2 + f_y^2}}$,

$N = \frac{f_{yy}}{\sqrt{1 + f_x^2 + f_y^2}}$, f_x and f_y are the first order partial derivatives

of $z=f(x, y)$ respect to x and y , respectively; f_{xx} and f_{yy} are the second order derivatives respect to x and y , respectively; f_{xy} is the second order mixed partial derivative respect to x and y ;

$$\Gamma_{11}^1 = 1/2 \cdot (G \cdot E_x - 2F \cdot F_x + F \cdot E_y) \cdot (E \cdot G - F^2)^{-1}$$

$$\Gamma_{11}^2 = 1/2 \cdot (2E \cdot F_x - E \cdot F_y + F \cdot E_x) \cdot (E \cdot G - F^2)^{-1}$$

$$\Gamma_{22}^1 = 1/2 \cdot (2G \cdot F_y - G \cdot G_x + F \cdot G_y) \cdot (E \cdot G - F^2)^{-1}$$

$$\Gamma_{22}^2 = 1/2 \cdot (E \cdot G_y - 2F \cdot F_y + F \cdot G_x) \cdot (E \cdot G - F^2)^{-1}$$

where E_x, F_x, G_x are partial derivatives of the E, F and G respect to x , and E_y, F_y, G_y are partial derivatives of the E, F and G respect to y .

Obtaining numerical solution of equations group above is a challenging task because it has the form of differential equation. Discretization is carried out through finite difference. After discretization, this equation group is converted to the iterative form for solution due to the large demanding computing time of direct methods compared with iterative numeric methods,

$$\begin{cases} \frac{f_{i+1,j}^{n+1} - 2f_{i,j}^{n+1} + f_{i-1,j}^{n+1}}{h^2} = \frac{L_{i,j}^n}{\sqrt{E_{i,j}^n + G_{i,j}^n - 1}} + \\ \frac{(\Gamma_{11}^1)_{i,j}^n \cdot (f_{i+1,j}^n - f_{i-1,j}^n) + (\Gamma_{11}^2)_{i,j}^n \cdot (f_{i,j+1}^n - f_{i,j-1}^n)}{2h} \\ \frac{f_{i,j+1}^{n+1} - 2f_{i,j}^{n+1} + f_{i,j-1}^{n+1}}{h^2} = \frac{N_{i,j}^n}{\sqrt{E_{i,j}^n + G_{i,j}^n - 1}} + \\ \frac{(\Gamma_{22}^1)_{i,j}^n \cdot (f_{i+1,j}^n - f_{i-1,j}^n) + (\Gamma_{22}^2)_{i,j}^n \cdot (f_{i,j+1}^n - f_{i,j-1}^n)}{2h} \end{cases} \quad (2)$$

where f_{ij}^n represents the result of $f(x, y)$ for the n^{th} iteration at (x_i, y_j) . $E_{i,j}^n$ and $G_{i,j}^n$ are the results of E and G for the n^{th} iteration at (x_i, y_j) ; $L_{i,j}^n$ and $N_{i,j}^n$ are the results of L and N for the n^{th} iteration at (x_i, y_j) , respectively. $(\Gamma_{11}^1)_{i,j}^n, (\Gamma_{11}^2)_{i,j}^n, (\Gamma_{22}^1)_{i,j}^n$ and $(\Gamma_{22}^2)_{i,j}^n$ are the corresponding results of the coefficients, for details the reader can refer to Yue (2011). h represents the step length for simulation; $n \geq 0$; $f_{0,j}^0, f_{i,0}^0, f_{M+1,j}^0, f_{i,M}^0$ are bound conditions, given $M+2$ as the grid number in x direction or y direction.

$f_{ij}^0 = f_{ij}$, and f_{ij} is interpolation according to \bar{f}_{ij} , which is the sampled value of f at the position (x_i, y_j) . Taking the sampled points as constraint conditions and convert equations group Eq.(2) to matrix form, we can formulate the following expressions,

$$\begin{cases} \min \left\| \begin{bmatrix} A \\ B \end{bmatrix} X^{n+1} - \begin{bmatrix} D^n \\ E^n \end{bmatrix} \right\| \\ \text{s. t. } S X^{n+1} = K \end{cases} \quad (3)$$

where $X^{n+1} = (f_{1,1}^{n+1}, \dots, f_{1,M}^{n+1}, \dots, f_{M,1}^{n+1}, \dots, f_{M,M}^{n+1})$; A and B represent the two coefficient matrices in the Eq.(1); D^n and E^n are the right side items of the two equations in matrix form, respectively. Finally, the solution of HASM can be converted to the solution of following expression,

$$FX^{n+1} = T^n \quad (4)$$

where

$$\begin{aligned} F &= [A^T \ B^T \ \lambda \cdot S^T] \begin{bmatrix} A \\ B \\ \lambda \cdot S \end{bmatrix}, \\ T^n &= [A^T \ B^T \ \lambda \cdot S^T] \begin{bmatrix} D^n \\ E^n \\ \lambda \cdot K \end{bmatrix}. \end{aligned}$$

2.2 Gauss-Seidel method and modified Gauss-Seidel method

Traditionally, GS is one of the effective numerical methods for the solution of large scale linear systems. It shows convergency when employed to solve positive definite linear system using GS. Therefore, it can be used to solve the HASM linear system. However, it converges in a much low speed. In order to achieve a faster convergence for GS, Ujević (2006) presented a modified GS method with a higher convergence speed. Chen (2010) introduced this method and implemented fast solving of HASM. According to Chen, et al. (2010), MGS has a significantly improved convergence.

2.3 Two dimensional double successive projection algorithm

From the point of view of projection technique, GS can be regard as one-dimensional projection method (Saad, 2003), while MGS can be regarded as one dimensional double successive projection method (Jing & Huang, 2008). Based on sufficient analysis of GS and MGS, Jing and Huang (2008) developed the two dimensional double successive projection method to solve the huge linear system. According to Jing and Huang (2008), the method of Ujević (2006) can be regarded as one dimensional double successive projection method, named 1D-DSPM, which has two independent subspaces to carry out projection calculation. Contrasted with 1D-DSPM, two dimensional double successive projection method, named 2D-DSPM, chooses the linear combination of subspaces, and hence to have enhanced performance. Thus, we can make following analysis by introducing projection technique:

According to Ujević (2006), we can get the Eq.(5) when solving general linear system $\mathbf{Ax} = \mathbf{b}$

$$\begin{cases} \mathbf{x}_{k+1} = \mathbf{x}_k + \alpha_1 \mathbf{v}_1 + \beta_2 \mathbf{v}_2 \\ f(\mathbf{x}_{k+1}) - f(\mathbf{x}_k) = -\frac{p_1^2}{2a} - \frac{(cp_1 - ap_2)^2}{2a^2 d} \end{cases} \quad (5)$$

where $k = 1, \dots, n$

$$\alpha_1 = -\frac{p_1}{a}, \beta_2 = \frac{cp_1 - ap_2}{ad}, f(\mathbf{x}) = \frac{1}{2} \langle \mathbf{Ax}, \mathbf{x} \rangle - \langle \mathbf{b}, \mathbf{x} \rangle,$$

$$a = \langle \mathbf{Av}_1, \mathbf{v}_1 \rangle, c = \langle \mathbf{Av}_1, \mathbf{v}_2 \rangle = \langle \mathbf{Av}_2, \mathbf{v}_1 \rangle,$$

$$d = \langle \mathbf{Av}_2, \mathbf{v}_2 \rangle, p_1 = \langle \mathbf{Ax}_k - \mathbf{b}, \mathbf{v}_1 \rangle, p_2 = \langle \mathbf{Ax}_k - \mathbf{b}, \mathbf{v}_2 \rangle$$

Eq.(5) can be derived through choosing subspaces in two successive steps. In the first step:

$\mathcal{K}_1 = \mathbf{L}_1 = \text{span} \{ \mathbf{v}_1 \}$, $\mathbf{x}_0 = \mathbf{x}_k$, $\tilde{\mathbf{x}}_{k+1} \in \mathbf{x}_k + \mathcal{K}_1$, should be figured out, given $\mathbf{b} - \mathbf{A}\tilde{\mathbf{x}}_{k+1} \perp \mathbf{L}_1$. Supposed $\tilde{\mathbf{x}}_{k+1} = \mathbf{x}_k + \tilde{\alpha}\mathbf{v}_1$, according to inner products, we can get $\tilde{\alpha} = -\frac{p_1}{a}$.

Similarly,

$\mathcal{K}_2 = \mathbf{L}_2 = \text{span} \{ \mathbf{v}_2 \}$, $\mathbf{x}_0 = \tilde{\mathbf{x}}_{k+1}$, $\mathbf{x}_{k+1} \in \tilde{\mathbf{x}}_{k+1} + \mathcal{K}_2$, should be calculated, with the condition $\mathbf{b} - \mathbf{A}\mathbf{x}_{k+1} \perp \mathbf{L}_2$. Suppose $\mathbf{x}_{k+1} = \tilde{\mathbf{x}}_{k+1} + \tilde{\beta}\mathbf{v}_2$, according to inner products, we can calculate $\tilde{\beta} = \frac{cp_1 - ap_2}{ad}$.

From aforementioned results, we can see both 1D-DSPM and MGS have the same result, hence belongs to a special projection method. The subspaces chosen by 2D-DSPM is linear combination of subspaces $\mathcal{K}_1, \mathcal{K}_2$ chosen in 1D-DSPM in two successive steps. That is, $\mathcal{K} = \mathbf{L} = \text{span} \{ \mathbf{v}_1, \mathbf{v}_2 \}$ should be find out, under the condition that $\mathbf{b} - \mathbf{A}\mathbf{x}_{k+1} \perp \mathbf{L}$, $\mathbf{x}_{k+1} \in \mathbf{x}_k + \mathcal{K}$, where $\mathbf{x}_{k+1} = \mathbf{x}_k + \alpha\mathbf{v}_1 + \beta\mathbf{v}_2$.

Similar to 1D-DSPM, according to inner products, we can get the following results:

$$\alpha = \frac{cp_2 - dp_1}{ad - c^2}, \beta = \frac{cp_1 - ap_2}{ad - c^2} \quad (6)$$

where a, c, d have the same meaning as Eq.(5), and we can choose $\mathbf{v}_1 = \mathbf{e}_i, \mathbf{v}_2 = \mathbf{e}_j; i \neq j$. It can be proved that 2D-DSPM has higher convergence rate than MGS in Ujević (2006). The overall 2D-DSPM can be described below.

```

For iternum=1,2,..., to maximum iterative times
//initialize
x=x_0
//for each row in linear system execute following loop
For i=1,2,...,n
//choose two subspaces first
j=i-ijgap
If i≤ijgap then
j=i-ijgap+n
Endif
//carry out 2D-DSPM method
pi=(ai,x)-bi
pj=(aj,x)-bj
μi=aiiajj-aij2
αi=aijpj-ajipi
μi
xi=xi+αi
βj=aijpi-aiipj
μi
xj=xj+βj
End for i
//update the linear system
x0=x
End for iternum

```

In the above algorithm, ij_{gap} represents the interval between subspace i and j , and other variables have the same meaning as Eq.(5).

3 IMPLEMENTATION AND VALIDATION

Amongst the aforementioned numerical methods, GS consumes the least memory. Compared with Jacobi method, GS

method can reduce half memory demanding since it does not need to save the two successive results calculated. Therefore, it can support the solution of relatively large linear systems even when the memory is not large. MGS accelerates the convergence speed with the same memory compared with GS. Furthermore, 2D-DSPM optimizes the selection of projection spaces and makes two corrections to the iterative results, and hence to obtain the obviously accelerated convergence speed.

The coefficient matrix can be found distributed in five-diagonal form through observation of its structure. Moreover, in each row, there are eight non-zero elements at most besides the diagonal entries. These elements distributed symmetrically with respect to the diagonal and elements have the fixed value in each line and distributed regularly. Implementation of our algorithm takes all these features into consideration to reduce the memory consumption, optimize the efficiency and reduce complexity of the program. We implemented these algorithms including GS, MGS and 2D-DSPM using C++ program language and nominated HASM-GS, HASM-MGS and HASM-DSPM, respectively.

To validate the effectiveness of HASM-DSPM, two experiments were designed. For the first experiment, a convergence analysis was carried out and execution time of these algorithms will be compared when simulating Gauss synthetic numerical surfaces. For the second experiment, the convergence rate, speed and accuracy for simulating a real-world example will be validated.

3.1 Gauss synthetic surface validation

Gauss synthetic surface was employed for simulation and performance analysis of HASM-DSPM. The Gauss synthetic surface selected can be presented as below:

$$f(x,y) = 3(1-x)^2 e^{-x^2-(y+1)^2} - 10(x/5 - x^3 - y^5) e^{-x^2-y^2} - e^{-(x+1)^2-y^2}/3 \quad (7)$$

where $f(x,y)$ represents the elevation of location (x,y) .

Two scales of grid numbers are chosen and they are 201×201 and 1001×1001 , respectively. The sizes of two grids are respectively 0.03 m and 0.06 m and the elevation both range from 8.10 m to -6.55 m. Fig. 1 shows the simulation results of HASM-GS, HASM-MGS and HASM-DSPM and for all three methods with the iteration of 1500. From the illustration, we can see the convergence rate of HASM-MGS is obvious speedup compared with HASM-GS. Furthermore, HASM-DSPM converges considerably faster than both HASM-GS and HASM-MGS, and can obtain a higher accuracy than HASM-GS and HASM-MGS with the same iteration. Additionally, it can be observed that when the iterative numbers are up to a particular number, the local fluctuation is obvious for HASM-GS, while HASM-DSPM fluctuates slightly and nearly is continuous convergent.

We established 1000 and 5000 as two iterative numbers, and the accuracy threshold for exiting iterative simulation as 10^{-16} . The test result in Table 1 indicated that for the same number of iteration the computing time of HASM-GS was considerably longer than HASM-GS, while HASM-DSPM was much less than the others. Furthermore, it is worth noticing that HASM-MGS used much more time than HASM-GS when simulating Gauss synthetic surface under conditions aforementioned, while HASM-DSPM spent the least time amongst all the methods. Taking

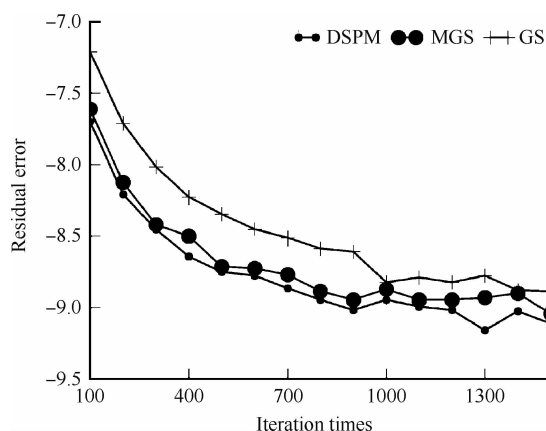


Fig.1 Convergence comparison of three methods

higher convergence rate into account, the simulation time of HASM-DSPM reduced considerably when achieving the same accuracy compared with HASM-MGS. Additionally, preconditioning needs extra computing time, which contributes to huge simulation time of HASM-MGS.

Table 1 Computing time of HASM-GS, HASM-MGS and HASM-DSPM

Grid number	Iteration number	HASM-GS/s	HASM-MGS/s	HASM-DSPM/s
40401	1000	6.132854	6.986757	5.731308
	5000	30.455048	34.891304	25.887218
1002001	1000	148.817963	172.805222	123.352486
	5000	743.159851	864.940369	614.852112

3.2 Poyang Lake basin simulation

Poyang Lake basin is located from $24^{\circ}29'14''N$ to $30^{\circ}04'41''N$ and from $113^{\circ}34'36''E$ to $118^{\circ}28'58''E$ in south-central China. It borders the Yangtze to the north and mountains to east, west and south. Its area is 166900 km^2 , of which mountainous areas account for 36%, hilly areas for 42% and plain and hillock areas for 12.1% and the water body area for 9.9%. Topography and geomorphology are complicated and appropriate for DEM simulation experiments. Data source is contours from Poyang Lake basin. Since the data scale is so huge, we have to partition it into 15 parts for simulation independently. Afterwards, discretization is made to all the parts to obtain scattered points as constrained conditions for HASM simulation. All these blocks were simulated employing HASM-GS, HASM-MGS and HASM-DSPM, respectively. Then the simulation results of computing time for 2000 iterations are given in Table 2.

From Table 2 we can see that for simulations of all the 15 blocks of Poyang Lake basin with the same iteration number, the computing time of MGS is much longer than GS due to additional preconditioning operation to speed up convergence; Among the three methods, DSPM has the shortest computing time, significantly shorter than MGS but slightly than GS. On the other side, due to the fastest convergence of DSPM, its efficiency improved significantly. When taking computing time of per iteration into account, DSPM decreased obviously compared with HASM-MGS. Although per iteration time for DSPM is slightly

Table 2 Computing time of Poyang Lake basin for three methods

Block Id	Grid number	HASM-GS/s	HASM-MGS/s	HASM-DSPM/s
1	2587×3196	2945.582	4443.372	3020.074
2	2514×1994	1786.494	2674.753	1924.369
3	2587×3040	2831.433	4223.551	3044.221
4	2587×3041	2813.467	4232.500	3021.856
5	2587×2595	2430.018	3620.767	2554.795
6	2587×3041	2818.938	4215.584	3338.053
7	2637×2850	2674.294	3991.656	2818.440
8	2562×2907	2658.301	3998.196	2773.491
9	1509×2535	1367.316	2041.357	1682.184
10	2289×2535	2075.806	3122.793	2272.787
11	2289×2513	2095.263	3094.257	2209.462
12	2562×3041	2786.372	4184.470	2891.475
13	2176×2370	1845.426	2773.477	1984.121
14	2587×3041	2812.212	4186.860	3189.935
15	2587×3028	2804.467	4216.730	2941.846

longer than that of HASM-GS, its convergence speed is much faster. Fig.2 reveals that contrasted with MGS, with the same iteration number, the computing time of HASM-DSPM could save computing time proportional to the first power of grid numbers.

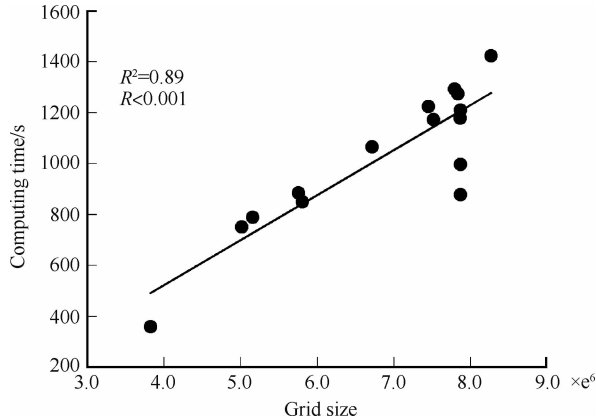


Fig.2 Relationship of residue of time and grid number for MGS and DSPM

Fig.3 shows the simulation time of all three methods when achieving the same accuracy 0.0542. The results illustrates that simulations of most blocks reached the certain accuracy before accomplishing all the iterations and exit in advance, except that the ID 1, ID 2, ID 3, ID 5, ID 11 iterated for the maximum times 2000. The analysis of the results demonstrates that DSPM method spent the least computing time, far less than GS and MGS. Even when performing the maximum iterations, DSPM still has the highest simulation speed and achieves the highest accuracy.

From Fig.2 and Fig.3, we can see that the computing time discriminates obviously between areas of approximately the same scale due to different processing time with different sampled points numbers.

In Table 3, the convergence of three methods are showed and compared for simulation of real-world example Poyang Lake basin and the iterative number is set as 2000. The simulation of all 15 partitions of Poyang Lake basin demonstrates the conclusion of Fig.1, which illustrates that when employed for real-world instance, HASM-DSPM has the superior convergence

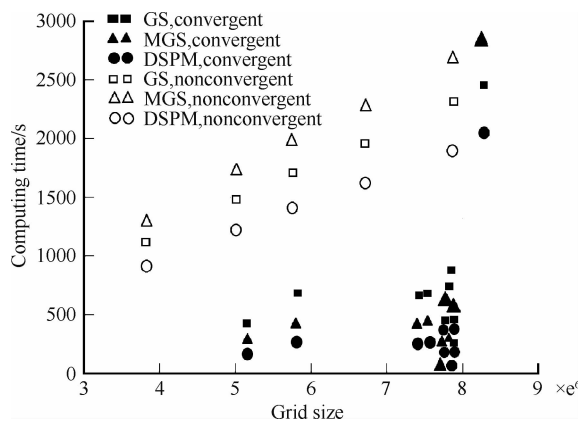


Fig.3 Simulation time spent when achieving the certain error threshold

rate over HASM-MGS and HASM-GS.

According to Fig.4, DSPM can reduce computing time considerably when attaining the same accuracy compared with GS and MGS.

Table 3 Simulation error of Poyang Lake basin with equal iteration number for three methods

Block ID	Grid number	HASM-GS/m	HASM-MGS/m	HASM-DSPM/m
1	2587×3196	0.058935	0.057806	0.057740
2	2514×1994	0.066383	0.065270	0.065226
3	2587×3040	0.060192	0.058382	0.058247
4	2587×3041	0.028442	0.024252	0.023840
5	2587×2595	0.072400	0.070647	0.070460
6	2587×3041	0.047883	0.041749	0.041372
7	2637×2850	0.042337	0.037377	0.036880
8	2562×2907	0.042449	0.038584	0.038295
9	1509×2535	0.057522	0.055217	0.055013
10	2289×2535	0.052051	0.050011	0.049867
11	2289×2513	0.067684	0.064961	0.064752
12	2562×3041	0.023237	0.018946	0.018630
13	2176×2370	0.040426	0.036316	0.036028
14	2587×3041	0.013206	0.010840	0.010636
15	2587×3028	0.043029	0.038002	0.037582

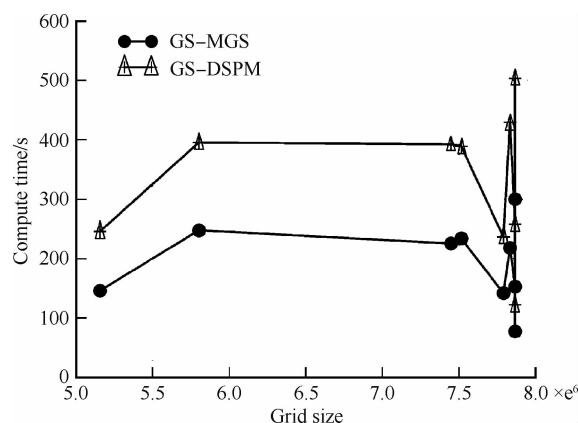


Fig.4 Relationship of time reduced and grid number between MGS and DSPM compared to each other

3.3 Accuracy comparison with other classical methods

One part of Poyang Lake basin is chosen for accuracy vali-

dation. The simulation result is compared with those of classical methods, such as TIN, KRIGING, SPLINE, and IDW, which is illustrated with Table 4. The area chosen for validation has 2684 × 2587 pixels, 40 m resolution and a height ranging from 36 to 2200 m. Sampled points for simulation and for validation have the same number 199442. RMSE is adopted to measure the error. Table 4 illustrates that HASM-DSPM has the highest accuracy.

Table 4 Simulation accuracy validation for HASM-DSPM /m

HASM-DSPM	TIN	KRIGING	SPLINE	IDW
17.594	18.704	26.799	20.399	20.891

4 CONCLUSION

A new method for solving HASM has been presented in this paper. Both numerical simulation and Poyang Lake basin simulation have verified that this method can attain improved simulation speed and convergence with the same memory capacity occupied, compared with HASM-GS and HASM-MGS. The simulation speed has improved greatly with the same error threshold matched. Furthermore, contrasted with other simulation methods, simulation results with HASM-DSPM have one meter's higher accuracy at least. RMSE was adopted as error measuring method. Additionally, since HASM-DSPM is a high performance method, and it gives a solution to large scale surface simulation.

REFERENCES

- Chen C F, Yue T X and Li Y Y. 2012. A high speed method of SMTS. *Computers & Geosciences*, 41: 64–71 [<http://dx.doi.org/10.1016/j.cageo.2011.08.012>]
- Chen C F, Yue T X and Liu H T. 2010. New method for solving high accuracy surface modeling. *Journal of Remote Sensing*, 14(4): 742–750
- Chen L J, Liu G H and Li H G. 2002. Estimating net primary productivity of terrestrial vegetation in China using remote sensing. *Journal of Remote Sensing*, 6(2): 129–135
- Hengl T and Evans I S. 2009. Mathematical and digital models of the land surface//Geomorphometry: Concepts, Software and Applications. Amsterdam: Elsevier: 31 – 63 [[http://dx.doi.org/10.1016/S0166-2481\(08\)00002-0](http://dx.doi.org/10.1016/S0166-2481(08)00002-0)]
- Jing Y F and Huang T Z. 2008. On a new iterative method for solving linear systems and comparison results. *Journal of Computational and Applied Mathematics*, 220(1–2): 74–84 [<http://dx.doi.org/10.1016/j.cam.2007.07.035>]
- Saad Y. 2003. Iterative Methods for Sparse Linear Systems. Boston: Philadelphia Society for Industrial Mathematics: 113–155
- Shi W J, Liu J Y, Du Z P, Song Y J, Chen C F and Yue T X. 2009. Surface modelling of soil pH. *Geoderma*, 150(1–2): 113–119 [<http://dx.doi.org/10.1016/j.geoderma.2009.01.020>]
- Ujević N. 2006. A new iterative method for solving linear systems. *Applied Mathematics and Computation*, 179(2): 725 – 730 [<http://dx.doi.org/10.1016/j.amc.2005.11.128>]
- Yue T X. 2011. Surface Modeling: High Accuracy and High Speed Methods. Boca Raton, FL: CRC Press: 103–135
- Yue T X and Du Z P. 2006. Numerical tests for optimal formulation of high accuracy surface modeling. *Geo-Information Science*, 8(3): 83–87
- Yue T X, Du Z P and Liu J Y. 2004. High precision surface modeling and error analysis. *Progress in Natural Science*, 14(3): 300–306
- Zhou Y, Qin Z H and Bao G. 2012. Land surface temperature estimation under cloud cover with GIDS. *Journal of Remote Sensing*, 16(3): 498–511

HASM 解算的 2 维双连续投影方法

闫长青^{1,2}, 岳天祥¹, 赵刚¹, 王晨亮¹

1.中国科学院 地理科学与资源研究所, 北京 100101;

2.山东科技大学 信息工程系, 山东 泰安 271000

摘要:基于曲面论原理的高精度曲面建模方法 HASM (High Accuracy surface Modelling)解决了长期困扰地理信息系统界的误差问题,但使用该方法需要求解大规模线性系统导致其计算效率较低,限制了其广泛应用。为提高 HASM 线性系统的解算速度和精度,本文基于 2 维双连续投影算法提出了一种解算 HASM 的新方法(HASM-DSPM),该方法采用选取优化的投影空间和两次校正策略以提高收敛速度和解算精度。理论分析表明,使用该方法比使用高斯赛尔方法 GS (Gauss-Seidel)和改进的高斯赛德尔方法 MGS (Modified Gauss-Seidel)效率明显提高。分别用本文引入的方法、高斯赛德尔方法和效率较高的 MGS 方法进行了 HASM 方程组的解算,并对高斯合成曲面和实际项目区进行了模拟试验。结果表明,与使用 GS、MGS 方法相比,HASM-DSPM 解算方法无论在收敛速度和计算时间方面都有明显改善,并且其模拟精度优于其他经典方法。

关键词:HASM, 2 维双连续投影, 曲面模拟, MGS 迭代, DEM

中图分类号:TP751.1

文献标志码:A

引用格式:闫长青,岳天祥,赵刚,王晨亮.2013. HASM 解算的 2 维双连续投影方法. 遥感学报,17(4): 717-727

Yan C Q, Yue T X, Zhao G and Wang C L. 2013. Two-dimensional double successive projection method for high accuracy surface modeling. *Journal of Remote Sensing*, 17(4): 717-727 [DOI: 10.11834/jrs.20132206]

1 引言

曲面模拟广泛地应用于地球表层模拟的各个方面,如气候(周义等,2012)、生态(陈利军等,2012; Shi 等,2009)和数字高程模型(DEM)模拟(Yue,2011)等。曲面模拟包括曲面采样、使用曲面模拟方法建立曲面和对所建立曲面进行精度评估 3 个阶段 (Hengl 和 Evans, 2009)。但由于现有的曲面模拟方法普遍缺乏完备的理论基础,导致模拟结果出现严重误差甚至错误。为了彻底解决曲面模拟方法的误差问题,岳天祥等(2004)、岳天祥 和 杜正平(2006)和 Yue(2011)发展并完善了基于微分几何曲面理论的高精度曲面模拟方法(HASM),解决了长期困扰地理信息系统界的模拟误差问题。该方法理论研究已趋于成熟,但由于使用该方法需求解大规

模线性方程组,速度问题制约了 HASM 在实时动态模拟以及大尺度、高分辨率 DEM 构建的应用。针对此问题,Yue(2011)采用多重网格算法来解算由 HASM 产生的大规模线性系统并发现此方法对高分辨率大尺度数据尤为适合;Chen 等人(2012)提出了一种改进的高斯赛德尔解算方法(MGS)来提高通过空间点位数据来构建 DEM 的效率。MGS 方法在不损失精度的前提下一定程度上加速了 DEM 的构建速度且该方法耗费内存较少,适合大规模的 DEM 模拟。

本文在研究分析 Chen 等人(2012)方法的基础上,引入空间投影技术,提出了一种基于 2 维双连续投影技术解算 HASM 的新方法(HASM-DSPM),并通过高斯合成曲面模拟和实际项目区 DEM 进行模拟证明了该方法的有效性。

收稿日期:2012-07-03;修订日期:2012-10-17;优先数字出版日期:2012-10-24

基金项目:国家杰出青年科学基金项目(编号:40825003);国家高技术研究发展计划(863 计划)(编号:2011AA120306);山东省优秀中青年科学家科研奖励基金(编号:BS2012HZ010);山东科技大学春蕾计划项目(编号:2010AZZ115)

第一作者简介:闫长青(1978—),男,博士研究生,现从事资源环境模型与系统模拟方面的研究。E-mail: yancq@lreis.ac.cn

通信作者简介:岳天祥(1963—),男,博士,研究员,从事发展以遥感数据或模型模拟数据为驱动场、以地面实测数据为优化控制条件的高精度高精度地球表层建模方法体系。E-mail: yue@lreis.ac.cn

2 基于 2 维双连续投影的高精度曲面解算方法

2.1 高精度曲面建模方法

高精度曲面方程基于微分几何曲面论,从曲面的确定因素入手,把曲面建模问题归结为对如下偏微分方程组的求解(Yue, 2011):

$$\begin{cases} f_{xx} = \Gamma_{11}^1 \cdot f_x + \Gamma_{11}^2 \cdot f_y + L \cdot (E \cdot G - f^2)^{-1/2} \\ f_{yy} = \Gamma_{22}^1 \cdot f_x + \Gamma_{22}^2 \cdot f_y + N \cdot (E \cdot G - f^2)^{-1/2} \end{cases} \quad (1)$$

式中, E 、 F 和 G 为第 1 类基本量, L 、 M 和 N 为第 2 类基本量, Γ_{11}^1 、 Γ_{11}^2 、 Γ_{22}^1 和 Γ_{22}^2 为联系系数, 其表达式分别为:

$$E = 1 + f_x^2, F = f_x \cdot f_y, G = 1 + f_y^2, L = \frac{f_{xx}}{\sqrt{1 + f_x^2 + f_y^2}},$$

$N = \frac{f_{yy}}{\sqrt{1 + f_x^2 + f_y^2}}$, f_x 和 f_y 分别为 $z=f(x, y)$ 对 x 和 y 的一阶偏导; f_{xx} 和 f_{yy} 为 $z=f(x, y)$ 分别对 x 和 y 的二阶偏导。

$$\Gamma_{11}^1 = 1/2 \cdot (G \cdot E_x - 2F \cdot F_x + F \cdot E_y) \cdot (E \cdot G - f^2)^{-1}$$

$$\Gamma_{11}^2 = 1/2 \cdot (2E \cdot F_x - E \cdot F_y + F \cdot E_x) \cdot (E \cdot G - f^2)^{-1}$$

$$\Gamma_{22}^1 = 1/2 \cdot (2G \cdot F_y - G \cdot G_x + F \cdot G_y) \cdot (E \cdot G - f^2)^{-1}$$

$$\Gamma_{22}^2 = 1/2 \cdot (E \cdot G_y - 2F \cdot F_y + F \cdot G_x) \cdot (E \cdot G - f^2)^{-1}$$

式中, E_x 、 F_x 、 G_x 为第 1 类基本量对 x 的一阶偏导; E_y 、 F_y 、 G_y 为第 2 类基本量对 y 的一阶偏导。

方程组式(1)求解时需离散化并转为迭代形式:

$$\begin{cases} \frac{f_{i+1,j}^{n+1} - 2f_{i,j}^{n+1} + f_{i-1,j}^{n+1}}{h^2} = \frac{L_{i,j}^n}{\sqrt{E_{i,j}^n + G_{i,j}^n - 1}} + \\ \frac{(\Gamma_{11}^1)_{i,j}^n \cdot (f_{i+1,j}^n - f_{i-1,j}^n) + (\Gamma_{11}^2)_{i,j}^n \cdot (f_{i,j+1}^n - f_{i,j-1}^n)}{2h} \\ \frac{f_{i,j+1}^{n+1} - 2f_{i,j}^{n+1} + f_{i,j-1}^{n+1}}{h^2} = \frac{N_{i,j}^n}{\sqrt{E_{i,j}^n + G_{i,j}^n - 1}} + \\ \frac{(\Gamma_{22}^1)_{i,j}^n \cdot (f_{i+1,j}^n - f_{i-1,j}^n) + (\Gamma_{22}^2)_{i,j}^n \cdot (f_{i,j+1}^n - f_{i,j-1}^n)}{2h} \end{cases} \quad (2)$$

式中, $f_{i,j}^n$ 表示 $f(x, y)$ 在网格点 (x_i, y_j) 第 n 次迭代得到的结果; $E_{i,j}^n$ 和 $G_{i,j}^n$ 分别是第 1 类基本量 E 和 G 在网格点 (x_i, y_j) 第 n 步迭代得到的结果; $L_{i,j}^n$ 和 $N_{i,j}^n$ 是第 2 类基本量 L 和 N 在网格点 (x_i, y_j) 第 n 次迭代后的结果; $(\Gamma_{11}^1)_{i,j}^n$ 、 $(\Gamma_{11}^2)_{i,j}^n$ 、 $(\Gamma_{22}^1)_{i,j}^n$ 和 $(\Gamma_{22}^2)_{i,j}^n$ 为相应系数的第 n 次迭代结果, 可参考文献(Yue, 2011); h 表示模拟步长; $n \geq 0$; $f_{0,j}^0, f_{i,0}^0, f_{M+1,j}^0, f_{i,M}^0$ 边界

条件,且假定 $M+2$ 为沿 x 或 y 方向的网格数目。 $f_{i,j}^0 = f_{i,j}$, $f_{i,j}$ 通过 $\bar{f}_{i,j}$ 插值得到, $\bar{f}_{i,j}$ 是 f 在采样点 (x_i, y_j) 的采样值。将采样点约束加入方程组并转化为矩阵表达形式可得:

$$\begin{cases} \min \left\| \begin{bmatrix} \mathbf{A} \\ \mathbf{B} \end{bmatrix} \mathbf{X}^{n+1} - \begin{bmatrix} \mathbf{D}^n \\ \mathbf{E}^n \end{bmatrix} \right\| \\ \text{s. t. } \mathbf{S} \mathbf{X}^{n+1} = \mathbf{K} \end{cases} \quad (3)$$

式中, $\mathbf{X}^{n+1} = (f_{1,1}^{n+1}, \dots, f_{1,M}^{n+1}, \dots, f_{M,1}^{n+1}, \dots, f_{M,M}^{n+1})$; \mathbf{A} 和 \mathbf{B} 分别表示式(2)的两个系数矩阵; \mathbf{D}^n 和 \mathbf{E}^n 分别为两矩阵方程的右端项。最后问题转化为

$$\mathbf{F} \mathbf{X}^{n+1} = \mathbf{T}^n \quad (4)$$

的线性系统求解。

式中,

$$\mathbf{F} = [\mathbf{A}^T \quad \mathbf{B}^T \quad \lambda \cdot \mathbf{S}^T] \begin{bmatrix} \mathbf{A} \\ \mathbf{B} \\ \lambda \cdot \mathbf{S} \end{bmatrix},$$

$$\mathbf{T}^n = [\mathbf{A}^T \quad \mathbf{B}^T \quad \lambda \cdot \mathbf{S}^T] \begin{bmatrix} \mathbf{D}^n \\ \mathbf{E}^n \\ \lambda \cdot \mathbf{K} \end{bmatrix}.$$

2.2 高斯赛德尔和改进的高斯赛德尔算法

GS 方法是求解大规模线性方程组的有效方法之一。理论证明,用 GS 求解正定线性系统是收敛的,可用于解算正定的 HASM 线性系统,但该方法收敛速度较慢。针对上述问题, Ujević(2006) 提出了一种收敛速度更快的改进高斯赛德尔方法(MGS)。陈传法等人(2010) 引入该方法实现了对高精度曲面建模方法的高速计算,根据其计算结果可知, MGS 方法收敛速度比 GS 方法显著提高。

2.3 2 维双连续投影算法

从投影技术的角度分析, GS 方法可以看做 1 维单连续投影方法(Saad, 2003), MGS 则可以看做是 1 维双连续投影方法(Jing 和 Huang, 2008)。在分析 GS 和 MGS 方法的基础上, Jing 和 Huang(2008) 建立了 2 维双连续投影(2D-DSPM)的线性系统求解方法。根据 Jing 和 Huang(2008) 理论推导, Ujević(2006) 的方法可看做 1 维双连续投影方法(1D-DSPM), 其求解过程分别选取两个独立的子空间进行投影计算。而 2D-DSPM 和其相比, 选取的投影计算子空间为 1D-DSPM 子空间的线性组合, 因而具有更快的迭代速度。引入投影技术对 MGS 方法分析如下:

当求解普通线性系统 $\mathbf{Ax} = \mathbf{b}$ 时,

由 Ujević(2006)方法可构造式(5)进行解算:

$$\begin{cases} \mathbf{x}_{k+1} = \mathbf{x}_k + \alpha_1 \mathbf{v}_1 + \beta_2 \mathbf{v}_2 \\ f(\mathbf{x}_{k+1}) - f(\mathbf{x}_k) = -\frac{p_1^2}{2a} - \frac{(cp_1 - ap_2)^2}{2a^2 d} \end{cases} \quad (5)$$

式中, $k=1, \dots, n$; $\alpha_1 = -\frac{p_1}{a}$, $\beta_2 = \frac{cp_1 - ap_2}{ad}$,

$$f(\mathbf{x}) = \frac{1}{2} \langle \mathbf{A}\mathbf{x}, \mathbf{x} \rangle - \langle \mathbf{b}, \mathbf{x} \rangle,$$

$$a = \langle \mathbf{A}\mathbf{v}_1, \mathbf{v}_1 \rangle, c = \langle \mathbf{A}\mathbf{v}_1, \mathbf{v}_2 \rangle = \langle \mathbf{A}\mathbf{v}_2, \mathbf{v}_1 \rangle,$$

$$d = \langle \mathbf{A}\mathbf{v}_2, \mathbf{v}_2 \rangle, p_1 = \langle \mathbf{A}\mathbf{x}_k - \mathbf{b}, \mathbf{v}_1 \rangle, p_2 = \langle \mathbf{A}\mathbf{x}_k - \mathbf{b}, \mathbf{v}_2 \rangle$$

\mathbf{v} 为单位向量, \mathbf{b} 为式(4)中的右端向量。

式(5)通过连续两步选取子空间得到, 对于两个子空间 \mathcal{K}_1 和 \mathcal{K}_2 分别计算如下:

$\mathcal{K}_1 = \mathbf{L}_1 = \text{span}\{\mathbf{v}_1\}$, $\mathbf{x}_0 = \mathbf{x}_k$, 令 $\mathbf{b} - \mathbf{A}\tilde{\mathbf{x}}_{k+1} \perp \mathbf{L}_1$, 求 $\tilde{\mathbf{x}}_{k+1} \in \mathbf{x}_k + \mathcal{K}_1$, 式中, $\tilde{\mathbf{x}}_{k+1} = \mathbf{x}_k + \tilde{\alpha}\mathbf{v}_1$, 由内积可求得 $\tilde{\alpha} = -\frac{p_1}{a}$, 同理:

$\mathcal{K}_2 = \mathbf{L}_2 = \text{span}\{\mathbf{v}_2\}$, $\mathbf{x}_0 = \tilde{\mathbf{x}}_{k+1}$, 令 $\mathbf{b} - \mathbf{A}\mathbf{x}_{k+1} \perp \mathbf{L}_2$, 求 $\mathbf{x}_{k+1} \in \tilde{\mathbf{x}}_{k+1} + \mathcal{K}_2$,

式中, $\mathbf{x}_{k+1} = \tilde{\mathbf{x}}_{k+1} + \tilde{\beta}\mathbf{v}_2$, 由内积可求得 $\tilde{\beta} = \frac{cp_1 - ap_2}{ad}$ 。

由此可见, 1 维双连续投影方法与 MGS 方法求得的近似解相同, 属于一种特殊的投影方法。而对于 2 维双连续投影方法, 每一次迭代选取的子空间为 1 维双连续投影方法每一步选取的两个子空间 \mathcal{K}_1 、 \mathcal{K}_2 的线性组合, 即 $\mathcal{K} = \mathbf{L} = \text{span}\{\mathbf{v}_1, \mathbf{v}_2\}$, 令 $\mathbf{b} - \mathbf{A}\mathbf{x}_{k+1} \perp \mathbf{L}$, 求 $\mathbf{x}_{k+1} \in \mathbf{x}_k + \mathcal{K}$, 式中 $\mathbf{x}_{k+1} = \mathbf{x}_k + \alpha\mathbf{v}_1 + \beta\mathbf{v}_2$ 同理由内积可求得

$$\alpha = \frac{cp_2 - dp_1}{ad - c^2}, \beta = \frac{cp_1 - ap_2}{ad - c^2} \quad (6)$$

式中, $\mathbf{v}_1 = \mathbf{e}_i, \mathbf{v}_2 = \mathbf{e}_j; i \neq j$ 。可以证明 2 维双连续投影方法收敛速度比 Ujević(2006) 提出的 MGS 方法快。由上述分析可得 2 维双连续投影方法(2D-DSPM)的实现算法:

```

For iterum=1,2,...,至最大迭代次数
//赋初值
x=x0
//对于线性系统中每一行执行如下 For 循环
For i=1,2,...,n
//先选取两个线性子空间
j=i-ijgap
if i<=ijgap then
j=i-ijgap+n
Endif

```

//执行双连续投影方法

$$p_i = (\mathbf{a}_i, \mathbf{x}) - b_i$$

$$p_j = (\mathbf{a}_j, \mathbf{x}) - b_j$$

$$\mu_i = a_{ii}a_{jj} - a_{ij}^2$$

$$\alpha_i = \frac{a_{ij}p_j - a_{ji}p_i}{\mu_i}$$

$$\mathbf{x}_i = \mathbf{x}_i + \alpha_i$$

$$\beta_j = \frac{a_{ij}p_i - a_{ii}p_j}{\mu_i}$$

$$\mathbf{x}_j = \mathbf{x}_j + \beta_j$$

End for i

//更新线性系统

$$\mathbf{x}_0 = \mathbf{x}$$

End for iterum

此算法段中 ij_{gap} 表示子空间 i 和 j 之间的间隔, n 表示矩阵的行数 0。

3 算法实现与验证

GS 方法与雅可比方法相比, 可以不用存储相邻两次计算结果, 节省了与求算未知矩阵相同空间的计算量, 从而对内存稀缺情况下的线性系统求解提供了有力支持。与 GS 方法相比, MGS 在保持相同存储空间的要求下加快了收敛速度。本文引入的 2D-DSPM 方法在 MGS 的基础上优化投影空间的选取并通过迭代结果进行两次校正使得收敛速度更快。

分析 HASM 方程组的系数矩阵可知其系数矩阵的中间部分呈块五对角分布, 且除去对角线元素外每行最多 8 个非零元素。这些非零元素关于对角线对称分布且每行的非零元素值呈规律分布, 即每行元素可以看作由其相邻的上方一行元素向右平移一个单位得到。本文算法实现时充分利用这些特点, 减少了内存耗费并优化程序执行的效率和复杂性。利用 C++ 语言实现了用 GS 方法、MGS 方法和 2D-DSPM 方法进行 HASM 方程求解的算法, 分别记为 HASM-GS、HASM-MGS 和 HASM-DSPM。

为了验证 HASM-DSPM 方法的效率, 设计了两个实验进行验证。实验一: 针对高斯合成曲面, 从算法的收敛性和同迭代次数时的执行时间对以上算法进行了对比分析。实验二: 针对实际项目区, 分别从收敛性、模拟速度和模拟精度 3 个方面进行了验证。

3.1 高斯合成曲面验证

通过高斯合成曲面对算法进行了测试, 曲面方程为:

$$f(x, y) = 3(1-x)^2 e^{-x^2-(y+1)^2} - 10(x/5 - x^3 - y^5) e^{-x^2-y^2} - e^{-(x+1)^2-y^2}/3 \quad (7)$$

式中, $f(x, y)$ 为 (x, y) 的高程值。本文采用的网格规模分别为 201×201 个网格和 1001×1001 个网格两种, 两者网格大小不同, 分别为 0.03 m 和 0.006 m , 高程范围相同, 最高高程与最低高程均分别为 8.10 m 和 -6.55 m 。图 1 列出 HASM-GS、HASM-MGS、HASM-DSPM、分别迭代 1500 次的收敛情况。由表 1 可见, 相对于 HASM-GS 算法, HASM-MGS 的收敛速度有较为明显提高。3 种方法中 HASM-DSPM 方法收敛速度最快, 且在相同迭代次数下所能达到的精度优于 HASM-GS 和 HASM-MGS。观察图 1 可知, 当迭代次数超过一定次数的时候 HASM-GS 出现了局部震荡的情况, 而此时 HASM-DSPM 震荡幅度最小接近持续收敛。

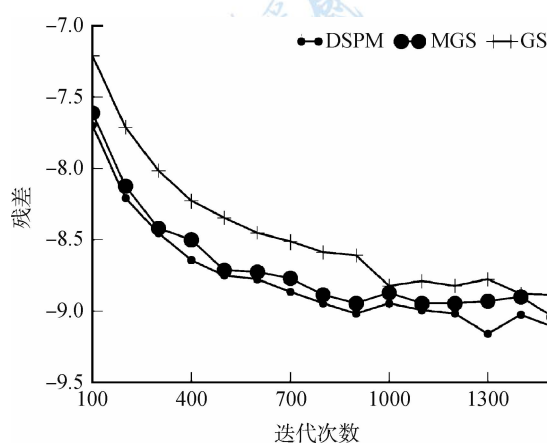


图 1 3 种方法收敛性比较

表 1 HASM-GS, HASM-MGS, HASM-DSPM 迭代时间

网格规模	迭代次数	HASM-GS/s	HASM-MGS/s	HASM-DSPM/s
40401	1000	6.132854	6.986757	5.731308
	5000	30.455048	34.891304	25.887218
1002001	1000	148.817963	172.805222	123.352486
	5000	743.159851	864.940369	614.852112

注: 误差精度为 10^{-16}

从表 1 可见, 完成相同的迭代次数 HASM-MGS 比 GS 耗费时间要多, 而 HASM-DSPM 消耗时间比二者都少; 对于高斯合成曲面的模拟, HASM-MGS

所耗费的时间明显大于 HASM-GS, 而 HASM-DSPM 方法所耗费的时间是三者中最少的。考虑到 HASM-DSPM 比收敛较快的 HASM-MGS 收敛速度还快, 使用 HASM-DSPM 方法完成模拟达到相同的误差所需时间会明显减少。而 HASM-MGS 之所以耗时较多, 是因为该方法需要预处理, 增加的额外预处理时间导致模拟时间增加。

3.2 鄱阳湖流域验证

鄱阳湖流域地处中国东南偏中部长江中下游南岸, 位于北纬 $24^{\circ}29'14''$ 至 $30^{\circ}04'41''$ 、东经 $113^{\circ}34'36''$ 至 $118^{\circ}28'58''$ 之间。鄱阳湖流域地势周高中低, 三面环山, 中部渐次由丘陵、盆地相间的地形向北成为平原。流域地貌类型以丘陵山地为主, 山地占 36%, 高丘 42%, 平原岗地约占 12.1%, 水面约占 9.9%。地形地貌较复杂, 适合 DEM 模拟试验。数据源为鄱阳湖流域的等高线, 因为数据量太大采用分块处理, 共分为 15 块, 等高线进行离散化后作为约束点集合以应用 HASM 模拟。用 HASM-GS、HASM-MGS 和 HASM-DSPM 分别模拟了鄱阳湖流域数字地面模型, 表 2 列出了 2000 次迭代次数下各种方法所耗费时间。

表 2 3 种算法同迭代次数模拟鄱阳湖时间

块号	网格规模	HASM-GS/s	HASM-MGS/s	HASM-DSPM/s
1	2587×3196	2945.582	4443.372	3020.074
2	2514×1994	1786.494	2674.753	1924.369
3	2587×3040	2831.433	4223.551	3044.221
4	2587×3041	2813.467	4232.500	3021.856
5	2587×2595	2430.018	3620.767	2554.795
6	2587×3041	2818.938	4215.584	3338.053
7	2637×2850	2674.294	3991.656	2818.440
8	2562×2907	2658.301	3998.196	2773.491
9	1509×2535	1367.316	2041.357	1682.184
10	2289×2535	2075.806	3122.793	2272.787
11	2289×2513	2095.263	3094.257	2209.462
12	2562×3041	2786.372	4184.470	2891.475
13	2176×2370	1845.426	2773.477	1984.121
14	2587×3041	2812.212	4186.860	3189.935
15	2587×3028	2804.467	4216.730	2941.846

从表 2 可知, 在设定的相同迭代次数下对于鄱阳湖流域的 15 块数据进行模拟时, MGS 耗费时间比 GS 方法多, 原因在于前者对于每个点均多做了一步预算计算处理以加快收敛; DSPM 所用模拟时间明显少于 MGS 而接近于 GS 方法, 但因收敛速度比 HASM-MGS 要明显加快因而效率得到极大提高。

而其单次迭代执行的时间比 HASM-MGS 明显降低,比 HASM-GS 增加并不明显,但其收敛速度远超出 HASM-GS。从图 2 可知,与 MGS 所消耗时间相比,HASM-DSPM 随着网格规模的增加执行相同迭代次数节省的时间也呈线性增加。

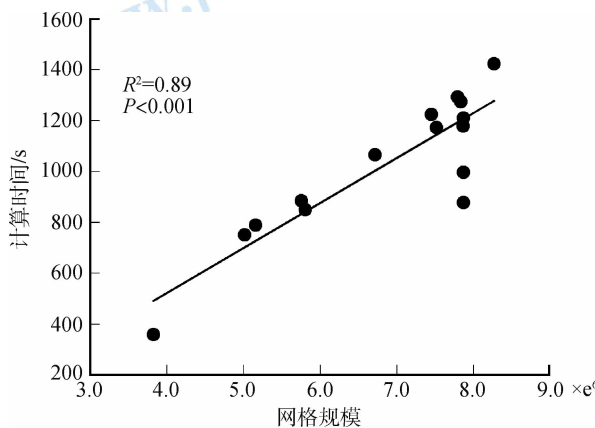


图 2 MGS 与 DSPM 方法时间差与网格规模的关系

图 3 给出了达到相同模拟误差阈值为 0.0542 时上述 3 种方法所用的时间,从表 2 中可见除了块号为 1、2、3、5、11 的 5 块因执行了相同的最大迭代次数 2000 未能达到模拟误差阈值,其余均达到该误差阈值终止退出。图 3 中可以观察到,DSPM 方法在达到该规定误差时所用时间最少,远小于 GS 和 MGS 方法;在执行到最大迭代次数时仍然是 DSPM 方法所用时间最少且精度最高。

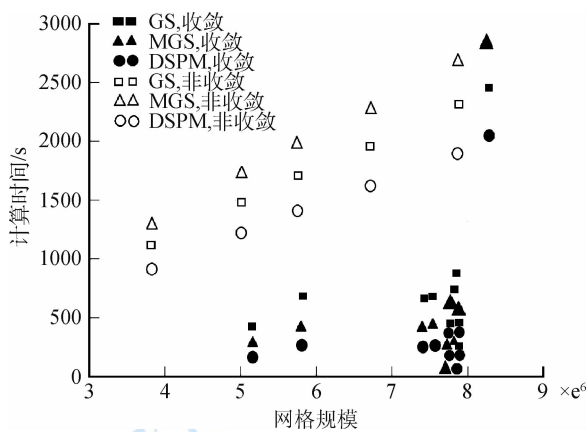


图 3 给定误差阈值所用的模拟时间

而由图 2 和图 3 可知,模拟网格规模相近的某些区域时模拟时间可能出现明显差别,其原因是 HASM 方法需要对采样点进行处理,采样点的数量对整个模拟时间有重要影响。

表 3 给出了模拟实际项目区鄱阳湖流域时达到

2000 次迭代次数时 3 种方法的收敛性比较。从表 3 中可以看出,鄱阳湖流域的 15 块数据的模拟情况均验证了图 1 的结论,说明对于实际项目区,HASM-DSPM 方法同样比 HASM-MGS 和 HASM-GS 收敛速度明显加快。

而由图 4 可知,在收敛到本文设定的误差精度时,以 GS 方法所耗费时间为参照 DSPM 方法相比 MGS 节省的时间有较大提高。

表 3 3 种方法模拟鄱阳湖同迭代次数误差

块号	网格规模	HASM-GS/m	HASM-MGS/m	HASM-DSPM/m
1	2587×3196	0.058935	0.057806	0.057740
2	2514×1994	0.066383	0.065270	0.065226
3	2587×3040	0.060192	0.058382	0.058247
4	2587×3041	0.028442	0.024252	0.023840
5	2587×2595	0.072400	0.070647	0.070460
6	2587×3041	0.047883	0.041749	0.041372
7	2637×2850	0.042337	0.037377	0.036880
8	2562×2907	0.042449	0.038584	0.038295
9	1509×2535	0.057522	0.055217	0.055013
10	2289×2535	0.052051	0.050011	0.049867
11	2289×2513	0.067684	0.064961	0.064752
12	2562×3041	0.023237	0.018946	0.018630
13	2176×2370	0.040426	0.036316	0.036028
14	2587×3041	0.013206	0.010840	0.010636
15	2587×3028	0.043029	0.038002	0.037582

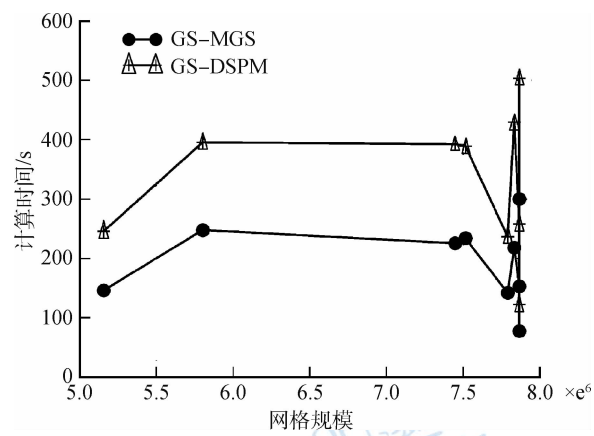


图 4 MGS 与 DSPM 方法时间差与网格规模的关系

3.3 HASM-DSPM 与经典方法的模拟精度比较

为了和经典曲面模拟方法精度对比,选取了鄱阳湖流域的一块区域进行精度验证。验证结果与经典插值方法不规则三角网(TIN)、克里金(KRIGING)、样条方法(SPLINE)和反距离加权方法(IDW)模拟精度进行了比较,结果如表 4 所示。该模拟区

域大小为 2684×2587 , 分辨率 40 m, 高程范围为 36—2200 m, 选取的模拟点和验证点的数量为 1:1, 均为 199442 个。误差度量采用均方根方法。

表 4 HASM-DSPM 方法模拟精度验证 /m

HASM-DSPM	TIN	KRIGING	SPLINE	IDW
17.594	18.704	26.799	20.399	20.891

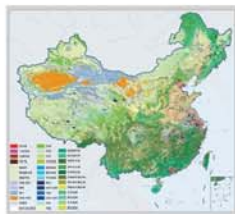
4 结 论

本文提出了一种解算 HASM 的新方法 HASM-DSPM。通过数值模拟和鄱阳湖流域模拟试验均证实,与 HASM-GS 和 HASM-MGS 相比 HASM-DSPM 在内存消耗相同的情况下,模拟速度和收敛速度比二者都有明显改善;在达到相同的收敛误差下, HASM-DSPM 的速度在 HASM-MGS 基础上又提高了接近一倍。同经典模拟方法的对比试验发现,使用 HASM-DSPM 方法对 DEM 模拟的均方根误差提高了至少 1 m 以上,可以达到最高的精度。而 DSPM 方法是一种高性能的解算方法,在一定程度上解决了 HASM 方程组求解的性能问题。

参考文献(References)

Chen C F, Yue T X and Li Y Y. 2012. A high speed method of SMTS.

- Computers & Geosciences, 41: 64–71 [<http://dx.doi.org/10.1016/j.cageo.2011.08.012>]
- 陈传法, 岳天祥, 刘洪涛. 2010. 高精度曲面模型解算改进的 Gauss-Seidel 法. 遥感学报, 14(4): 742–750
- 陈利军, 刘高焕, 励惠国. 2002. 中国植被净第一性生产力遥感动态监测. 遥感学报, 6(2): 129–135
- Hengl T and Evans I S. 2009. Mathematical and digital models of the land surface//Geomorphometry: Concepts, Software and Applications. Amsterdam: Elsevier: 31–63 [[http://dx.doi.org/10.1016/S0166-2481\(08\)00002-0](http://dx.doi.org/10.1016/S0166-2481(08)00002-0)]
- Jing Y F and Huang T Z. 2008. On a new iterative method for solving linear systems and comparison results. Journal of Computational and Applied Mathematics, 220(1–2): 74–84 [<http://dx.doi.org/10.1016/j.cam.2007.07.035>]
- Saad Y. 2003. Iterative Methods for Sparse Linear Systems. Boston: Philadelphia Society for Industrial Mathematics: 113–155
- Shi W J, Liu J Y, Du Z P, Song Y J, Chen C F and Yue T X. 2009. Surface modelling of soil pH. Geoderma, 150(1–2): 113–119 [<http://dx.doi.org/10.1016/j.geoderma.2009.01.020>]
- Ujević N. 2006. A new iterative method for solving linear systems. Applied Mathematics and Computation, 179(2): 725–730 [<http://dx.doi.org/10.1016/j.amc.2005.11.128>]
- Yue T X. 2011. Surface Modeling: High Accuracy and High Speed Methods. Boca Raton, FL: CRC Press: 103–135
- 岳天祥, 杜正平. 2006. 高精度曲面建模最佳表达形式的数值实验分析. 地球信息科学, 8(3): 83–87
- 岳天祥, 杜正平, 刘纪远. 2004. 高精度曲面建模与误差分析. 自然科学进展, 14(3): 300–306
- 周义, 覃志豪, 包刚. 2012. GIDS 空间插值法估算云下地表温度. 遥感学报, 16(3): 498–511



封面说明

About the Cover

2010年中国土地覆被遥感监测数据集 (ChinaCover2010)
The China National Land Cover Data for 2010 (ChinaCover2010)

2010年中国土地覆被遥感监测数据集 (ChinaCover2010) 由中国科学院遥感与数字地球研究所联合其他9个单位历时两年完成，应用30 m空间分辨率的环境星(HJ-1A/1B)数据，利用联合国粮农组织(FAO)的LCCS分类工具，构建了适用于中国生态特征的38类土地覆被分类系统，采用基于超算平台的数据预处理、面向对象的自动分类、地面调查获得的10万个野外样本以及雷达数据辅助分类相结合的方法，数据精度达到85%。ChinaCover2010主要基于国产卫星影像，将遥感与生态紧密结合，充足的野外样点以及严格的产品质量控制在最大程度上保证了数据的精度，可为中国生态环境变化评估以及生态系统碳估算提供基础数据支撑。(网址：<http://www.chinacover.org.cn>)

The China National Land Cover Data for 2010 (ChinaCover2010) has been completed after two years of team effort by the Institute of Remote Sensing and Digital Earth (RADI), Chinese Academy of Sciences (CAS), together with nine other institutions' participation. The HJ-1A/1B satellite at 30 m resolution is main data source. Based on the landscape features in China, 38 land cover classes have been defined using UN FAO Land Cover Classification System (LCCS). Super computers were used in the data preprocessing. An object-oriented method and a thorough field survey (about 100000 field samples) were used in the land cover classification, with radar imagery as auxiliary data. The overall accuracy of ChinaCover2010 is around 85%. Mainly based on domestic imagery, the products take advantage of various in situ data and strict quality control. ChinaCover2010 is a good dataset for ecological environment change assessment and terrestrial carbon budget studies. (Website: <http://www.chinacover.org.cn>)

遥感学报

JOURNAL OF REMOTE SENSING

YAOGAN XUEBAO (双月刊 1997年创刊)

第17卷 第4期 2013年7月25日

(Bimonthly, Started in 1997)

Vol.17 No.4 July 25, 2013

主 管	中国科学院	Superintended	by	Chinese Academy of Sciences
主 办	中国科学院遥感与数字地球研究所 中国地理学会环境遥感分会	Sponsored	by	Institute of Remote Sensing and Digital Earth,CAS The Associate on Environment Remote Sensing of China
主 编	顾行发	Editor-in-Chief		GU Xing-fa
编 辑	《遥感学报》编委会 北京市安外大屯路中国科学院遥感与数字地球研究所 邮编：100101 电话：86-10-64806643 http://www.jors.cn E-mail:jrs@irs.ac.cn	Edited	by	Editorial Board of Journal of Remote Sensing Add: P.O.Box 9718, Beijing 100101, China Tel: 86-10-64806643 http://www.jors.cn E-mail: jrs@irs.ac.cn
出 版	科学出版社	Published	by	Science Press
印 刷	北京科信印刷有限公司	Printed	by	Beijing Kexin Printing Co. Ltd.
总 发 行	科学出版社 北京东黄城根北街16号 邮政编码：100717 电话：86-10-64017032 E-mail:sales_journal@mail.sciencep.com	Distributed	by	Science Press Add: 16 Donghuangchenggen North Street, Beijing 100717, China Tel: 86-10-64017032 E-mail: sales_journal@mail.sciencep.com
国 外 发 行	中国国际图书贸易总公司 北京399信箱 邮政编码：100044	Overseas distributed	by	China International Book Trading Corporation Add: P.O.Box 399, Beijing 100044, China

中国标准连续出版物号：ISSN 1007-4619

CN 11-3841/TP

CODEN YXAUAB

国内邮发代号：82-324

国外发行代号：BM 1002

定价：70.00元

ISSN 1007-4619

国内外公开发行

